



Evaluation of the near-surface wind field over the Adriatic region: local wind characteristics in the convection-permitting model ensemble

Andreina Belušić Vozila¹ · Danijel Belušić^{2,3} · Maja Telišman Prtenjak² · Ivan Güttler⁴ · Sophie Bastin⁵ · Erwan Brisson⁶ · Marie-Estelle Demory⁷ · Andreas Dobler⁸ · Hendrik Feldmann⁹ · Øivind Hodnebrog¹⁰ · Stergios Kartsios¹¹ · Klaus Keuler¹² · Torge Lorenz¹³ · Josipa Milovac¹⁴ · Emanuela Pichelli¹⁵ · Mario Raffa¹⁶ · Pedro M. M. Soares¹⁷ · Merja H. Tölle¹⁸ · Heimo Truhetz¹⁹ · Hylke de Vries²⁰ · Kirsten Warrach-Sagi²¹

Received: 6 May 2022 / Accepted: 3 February 2023 / Published online: 28 February 2023
© The Author(s), under exclusive licence to Springer-Verlag GmbH Germany, part of Springer Nature 2023

Abstract

We present the first evaluation of the wind field from the ensemble of kilometer-scale simulations from the CORDEX-Flagship Pilot Study on convection, with focus on the Adriatic region. Kilometer-scale climate models, also known as convection-permitting models (CPMs), produce a good representation of small-scale topographic features and consequently a more detailed depiction of dynamical and thermal circulations. These enable a reliable view of climate characteristics of the wind field, especially in coastal regions and over complex terrain, such as the Adriatic region. We investigate the (potential) added value introduced by CPMs compared to classical “cumulus-parametrized” regional climate models (RCMs), reanalysis and station observations. For this purpose, wind components at 10 m level are used at 3-hourly frequency. All simulations cover a 10-year period, extending from 2000 to 2009. In terms of the standard statistical parameters such as correlation coefficient and temporal standard deviation, CPMs are very dependent on their parent RCM performance. However, the orographic forcing emphasizes the potential added value and CPMs contain some fine spatial scale variability (i.e., stronger extremes by 25% and more accurate wind direction) that is absent in coarser RCMs and reanalysis. The potential added value is higher in the cold season compared to the warm season due to the proportion of severe wind events. CPMs reproduce well the typical wind regimes along the Adriatic coast, namely Bora and Sirocco. The benefit of using CPMs is especially pronounced in simulating Bora maximum wind speeds in northern Adriatic and Sirocco frequencies in southern Adriatic. Based on our overall analysis, we conclude that CPMs provide added value compared to coarser models, especially in the complex coastal terrain.

Keywords Adriatic · Bora · Convection-permitting models · CORDEX · Regional climate models · Sirocco

1 Introduction

Evaluation of the wind field over complex terrain provides an excellent opportunity to assess the reliability of climate model simulations. However, it is a challenging task due to the limited accessibility of observational data and high variability in both wind speed and direction. Extensive studies comparing the modeled and observed climate characteristics of the wind field over particular parts of the Mediterranean region, where winds are strongly affected by the topography (e.g., Ulbrich et al. 2012), are still rare (Belušić et al. 2018;

Bonaldo et al. 2017; Obermann et al. 2016), especially on a sub-daily scale. However, sub-daily wind data are crucial in detecting the most severe wind events. Therefore, the evaluation of high-resolution climate models on sub-daily scales, in coastal regions and over complex terrain such as the Adriatic, can reveal whether they achieve a good representation of small-scale topographic features and hence more details in dynamical aspects. Moreover, the evaluation of the wind for the present climate is needed for building confidence in wind field projections over future decades.

Until recently, the highest horizontal resolution of coordinated regional climate simulations over Europe was 0.11° (~ 12 km), produced within the Coordinated Regional climate Downscaling Experiment (CORDEX; Jacob et al. 2020; Ruti et al. 2016; Somot et al. 2011). Belušić Vozila

✉ Andreina Belušić Vozila
andreina@iptpo.hr

Extended author information available on the last page of the article

et al. (2019) have analyzed the future wind field projections using a multi-model ensemble composed of CORDEX regional climate models (RCMs) for the Adriatic region, which previously showed a good performance when compared to the daily observed wind (Belušić et al. 2018). However, there is still space left for improvements, especially over the complex coastal region, where local winds often reach severe speeds due to the interaction with coastal topography and can be substantially variable along the coast and during 24 h.

With the recent proliferation of climate simulations using convection permitting models (CPMs) with grid spacing of ~ 3 km, an increasing number of studies shows considerable improvements in their representation of local and regional climate (e.g., Adinolfi et al. 2021; Ban et al. 2014, 2015, 2021; Kendon et al. 2021; Meredith et al. 2020; Pichelli et al. 2021). Such studies have investigated principally precipitation and have revealed that CPMs show significant advantages in representing complex orographic regions, in producing high-order statistics and predicting events with small temporal and spatial scales compared to RCMs (e.g., Gutowski et al. 2020) and reanalysis (e.g., Belušić et al. 2018). The aim of this paper is to study the capabilities of CPMs to realistically simulate the small-scale characteristics of local winds, with the focus on the Adriatic Bora (Grisogono and Belušić 2009) and Sirocco winds (Horvath et al. 2008; Pasarić et al. 2007) which were not captured well by the EURO-CORDEX simulations analyzed in Belušić et al. (2018).

The international coordinated framework CORDEX Flagship Pilot Study (FPS) on convective phenomena over Europe and the Mediterranean produced the first multi-model ensemble of convection permitting simulations (Ban et al. 2021; Coppola et al. 2020; Pichelli et al. 2021). There are 22 modeling groups and six non-hydrostatic regional climate models with a high output temporal resolution of 1-h and a grid spacing less or equal to 3 km. A large part of the simulations for the present-day climate driven by ERA-Interim reanalysis (Dee et al. 2011) have been completed and, therefore, will be considered here. A multi-model and multi-physics ensemble such as the CORDEX FPS gives a great opportunity to examine the added value in two ways; (i) to detect the potential added value introduced by CPMs compared to the parent RCMs and reanalysis and (ii) to perform in-situ statistical analysis of CPMs with respect to observations. In this study the wind field of the convection permitting CORDEX FPS ensemble is evaluated, with the focus on the Adriatic region. Accordingly, special attention is given to the comparison of the spatial variability of the wind speed and frequency distribution of wind directions in CPMs and RCMs.

Given that the focus of this study is on Bora and Sirocco, it is important to note that they are driven by two different

mechanisms. While Bora is a gusty downslope wind, which experiences a strong influence of the terrain and usually blows perpendicular to the Dinaric Alps, Sirocco is generated by synoptic-scale events and usually parallel to the coastline. The climatology of the present-day Bora wind, which is obtained from observations at meteorological stations (Poje 1992), from satellites (Zecchetto and Cappa 2001), and from simulations (Horvath et al. 2011; Prtenjak et al. 2015; Stiperski et al. 2012), reveals that Bora wind is the strongest, most frequent, and persistent over the northeastern Adriatic (i.e., the region around Trieste and Senj). The main characteristic of the Bora wind is the spatial variation in wind speed (Grisogono and Belušić 2009; Prtenjak et al. 2015) due to the formation of alternating Bora jets and wakes along the coast (e.g., Grubišić 2004; Večenaj et al. 2012). The wind speed often reaches severe intensities (i.e., maximum mean hourly wind speed $> 17.0 \text{ ms}^{-1}$, Bajić 1989) within the jets. These jets are associated with mountain passes (Kuzmić et al. 2013), which affect the Bora wind duration and strength locally. Contrary to the Bora wind, Sirocco is less influenced by the coastal orography. However, Sirocco is stronger along the eastern than along the western Adriatic coast, due to the channeling effects of the surrounding mountains (Pasarić et al. 2007). The maximum wind speeds are lower than for Bora, and the occurrence is less frequent than that of Bora events (Belušić et al. 2018). Long-term wind observations (Penzar et al. 2001; Poje 1992) indicate that Sirocco is more frequent and intense over the southern Adriatic than northward of the city of Split.

In order to address the mentioned objectives, we use an ensemble of 17 CPM simulations performed with four different non-hydrostatic models at ~ 3 km spatial scale, and 14 corresponding RCM simulations including five different models with horizontal resolution ranging from ~ 12 km to ~ 15 km. Moreover, we perform a location-based comparison of the simulations with several observational stations and ERA5 reanalysis data. All simulations and measurements cover a 10 year-long evaluation period extending from 2000 to 2009 with 3-h frequency. Four main points are addressed in this paper, which could emphasize the (potential) added value in both the wind speed and wind direction:

- (i) Spatial variability.
- (ii) Intense wind speeds.
- (iii) Wind roses.
- (iv) Chronology of events.

2 Data and methods

2.1 Climate model data

A CPM and a parent RCM are limited-area models, which typically share the majority of their main physical

components. The main difference between them is the removal of parametrization of deep convection in CPMs (Ban et al. 2014). Near-surface wind components at 10 m level were available at hourly frequency for both CPMs and RCMs, but 3-h data were extracted due to the availability of observations. All simulations cover a 10-year period, extending from 2000 to 2009. The initial conditions, lateral boundary conditions and sea surface temperatures were obtained from the ERA-Interim reanalysis; however, most of the CPM simulations were forced by an intermediate simulation (RCM parent domain). Each simulation is identified by the number indicated in the first column of Table 1.

2.1.1 Convection-permitting simulations

The CORDEX FPS convection permitting simulations (Coppola et al. 2020), performed over the ALP-3 domain (Adinolfi et al. 2021, see their Fig. 1) are used to investigate wind characteristics over the Adriatic. The ALP-3 domain is characterized by a spatial resolution of around 3 km (details about grid spacing can be found in Table 1) and spans an extended Alpine region from central Italy to northern Germany (4.56°W–17.40°E; 37.50°N–52.63°N). The Adriatic domain used for the analysis covers the entire Adriatic coastal area, Croatia and the neighboring

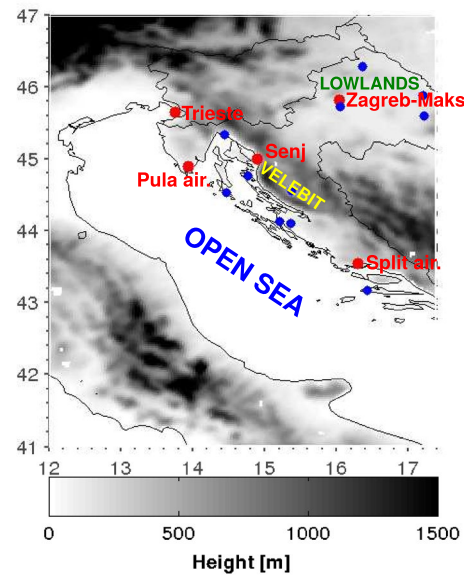


Fig. 1 Adriatic domain with stations analyzed in this study in dots. Names in red are associated with the stations mentioned in text. Gray shading indicates the topographic elevation in meters obtained from ICTP-RegCM4.7 CPM simulation

Table 1 Overview of the analyzed RCM and CPM simulations

Numbers	CPM	CPM grid (km)	Parent RCM	RCM grid (km)	Institution	Abbreviation (used in Fig. 3)
1	CNRM-AROME41t1	2.5	CNRM-ALADIN62	12.5	National Centre for Meteorological Research	CNRM
2	HCLIM38-AROME	2.5	RACMO23E	12.5	Royal Netherlands Meteorological Institute	KNMI
3	HCLIM38-AROME	3	HCLIM38-ALADIN	13	HARMONIE-Climate community: Danish Meteorological Institute and MET Norway and Swedish Meteorological and Hydrological Institute	HCLIMcom
4	COSMO-CLM	3	3-h data not available		Brandenburg University of Technology	BTU
5	COSMO-CLM	3	COSMO-CLM	12.5	Euro-Mediterranean Center on Climate Change	CMCC
6	COSMO-crCLIM	2.2	COSMO-crCLM	12.5	Swiss Federal Institute of Technology	ETH
7	COSMO-CLM	3	3-h data not available		University of Kassel	UKa
8	COSMO-CLM	3	3-h data not available		Karlsruhe Institute of Technology	KIT
9	RegCM4.7	3	RegCM4.7	12	International Centre for Theoretical Physics	ICTP
10	WRF381BG	3	WRF381BG	15	Aristotle University of Thessaloniki	AUTH
11	WRF381BF	3	WRF381BF	15	Bjerknes Centre for Climate Research	BCCR
12	WRF381BJ	3	WRF381BJ	15	Center for International Climate Research	CICERO
13	WRF381BH	3	WRF381BH	15	Instituto Dom Luiz	IDL
14	WRF381BE	3	WRF381BE	15	Institut Pierre Simon Laplace	IPSL
15	WRF381BI	3	WRF381BI	15	Universidad de Cantabria	UCAN
16	WRF381BD	3	WRF381BD	15	University of Hohenheim	UHOH
17	WRF381BL	3	WRF381BL	15	Wegener Center for Climate and Global Change	WEGC

countries (12–17.4°E, 41–47°N; Fig. 1). However, due to the availability of observations (see Sect. 2.3), the focus here is only on Croatia.

Four different models were considered: two configurations of AROME, namely CNRM-AROME41t1 (Fumière et al. 2020) and HCLIM38-AROME (Belušić et al. 2020), two configurations of COSMO, namely COSMO-CLM—Consortium for Small Scale Modeling (Baldauf et al. 2011; Rockel et al. 2008) and COSMO-crCLIM (Leutwyler et al. 2017; Schär et al. 2020), RegCM4.7—Regional Climate Modeling system (Coppola et al. 2021; Giorgi et al. 2012) and WRF—the Weather Research and Forecasting modeling system (Powers et al. 2017; Skamarock et al. 2019). Overall, 17 simulations are examined forming a multi-model convection-permitting ensemble (Table 1). A detailed description of each simulation can be found in Ban et al. (2021).

2.1.2 Regional climate simulations

In order to inspect the potential added value of a CPM simulation, the parent RCM simulation (Table 1) was also analyzed over the same domain (Fig. 1). The RCM horizontal grid spacing varies between 12 and 15 km. Five different models were considered: two configurations of ALADIN, namely CNRM-ALADIN62 (Colin et al. 2010) and HCLIM38-ALADIN (Belušić et al. 2020), COSMO-CLM, RACMO23 (Van Meijgaard et al. 2008), RegCM4.7 and WRF. The mentioned RCMs are implemented by several institutions and, therefore, form an ensemble of 14 RCM simulations. Two COSMO-CLM parent simulations are missing since the corresponding 3-h data was not available at the time this research was conducted, while one COSMO-CLM simulation downscaled ERA-Interim directly with the CPM without an intermediate simulation.

2.2 ERA5 reanalysis

The global reanalysis ERA5 (Hersbach et al. 2020) is the fifth generation ECMWF atmospheric reanalysis of the global climate extending from January 1950 to present, produced by the Copernicus Climate Change Service (C3S). The data is given on a 0.25° (~30 km) horizontal grid. Although available hourly, we use only the 10-m wind components at 3-h intervals from 2000 to 2009 in order to be analogous with the CPMs, RCMs and observations. ERA5 is also confronted to observations in the same way as CPMs and RCMs are. The objective for including ERA5 is to examine the potential added value of CPMs and to disclose its limitations for eventual near-surface wind evaluation.

2.3 Station observations

Station observations of wind speed and direction are used for validation purposes. While individual station observations are not always representative for the model grid cell, especially in the complex terrain, no high-quality gridded wind observational product is available for the selected Adriatic domain.

Wind observations at 10-m above ground level from 2000 to 2009 were gathered from different databases in SYNOP format, mostly from the Croatian Meteorological and Hydrological Service (DHMZ) and Croatia control (Crocontrol) and a few from NCDC-NOAA (Smith et al. 2011). Only stations having more than 70% of the 3-h data available in the period of interest are considered. Ultimately, a subset of 16 stations satisfied the criteria for both wind speed and direction and they are analyzed in this paper (Fig. 1). Each observational station is linked to the simulation grid cell whose center is the closest to it (in longitude and latitude) in order to evaluate the wind climatology.

2.4 Methods

The present-day climate wind evaluation is performed by computing the wind vector seasonal mean for DJF and JJA over the domain of interest. Wind vectors are computed using seasonal averages of u and v wind components and then decomposed into wind magnitude and direction. Probability density functions (PDFs) of the wind magnitude are examined and are complemented by calculating the Perkins skill score (PSS, Perkins et al. 2007), which measures a similarity between two PDFs by computing the common area between them. Additionally, special attention is given to the upper percentiles of the wind magnitude by focusing on the frequency distribution of the spatial 95th (Q95) percentile. The procedure for the latter includes the calculation of the spatial Q95 over the domain. Repeating this for each time step over the whole period of interest, we obtain the probability distribution of Q95. Finally, we find the frequency of occurrence for the spatial Q95 greater than 5 or 15 ms^{-1} . To assess the specific local wind regimes over the Adriatic two directional ranges are analyzed in detail following Belušić Vozila et al. (2019, 2021): i) perpendicular to the along-shore mountains NNE (22.5°)–ENE (67.5°) and ii) parallel with the alongshore mountains ESE (112.5°)–SSE (157.5°), which correspond to Bora and Sirocco directions, respectively. The direction ranges are selected in order to focus on the channeling effects of the terrain on both wind types. The Bora/Sirocco events are defined as the occurrence of 3-h wind from the respective directions. We also compare the standard statistical measures in the time domain (i.e., bias, standard deviation and correlation coefficient) between the simulations and in-situ observations divided in two groups,

namely inland and coastal stations. Finally, performances of individual models and dispersion of the ensemble is addressed for each presented score in order to identify differences among CPMs.

3 Results and discussion

3.1 The spatial variability

Figures 2 and 3 display the seasonal (DJF and JJA) mean normalized wind vectors and scalar wind speeds over the Adriatic for the CPM ensemble (a), RCM ensemble (b) and ERA5 reanalysis (c). The JJA season (Fig. 3) is less

windy than the DJF season (Fig. 2), and the JJA wind intensity differs less between land and open sea. Still, the wind speed over the sea is greater in both seasons, revealing the dominant wind regimes. The wind direction over the coast and sea is dominantly NE (Bora) in DJF. In JJA, E-SE flow occurs in the northern part of the domain and NW flow in the southern part, which strengthens towards the south. The latter is an indication of the Etesian wind (Tyrlis and Lelieveld 2013) which is observed in the warm season in the south Adriatic. The potential added value of dynamical downscaling to finer grid spacing can immediately be recognized from much more detailed structures in the spatial wind patterns (Figs. 2a and 3a).

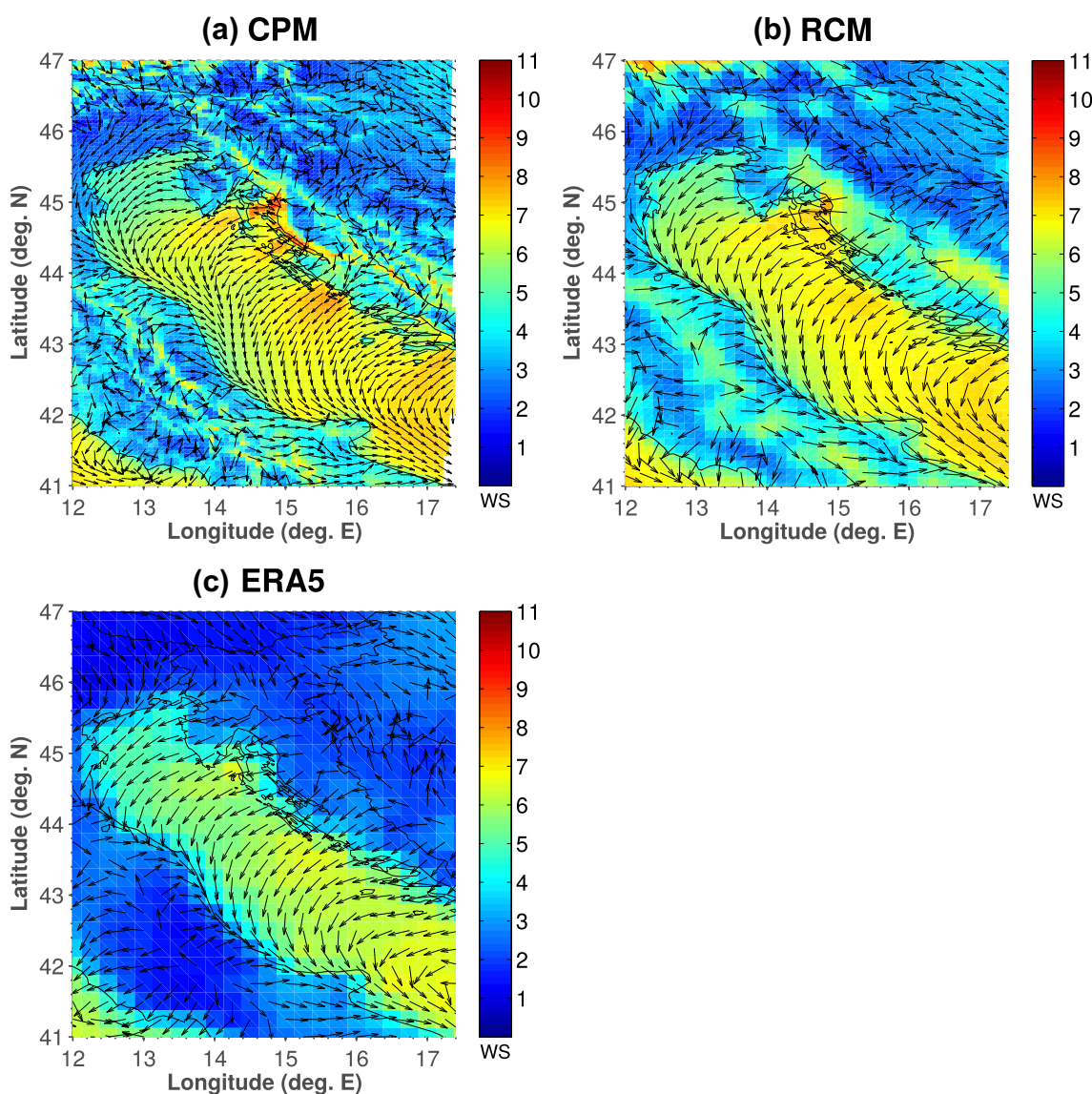


Fig. 2 Winter (DJF) mean of wind speed (colors) and normalized wind direction (black arrows) for **a** CPM ensemble mean, **b** RCM ensemble mean, **c** ERA5. For the CPM ensemble every 6th, while for the RCM ensemble every 2nd vector is shown

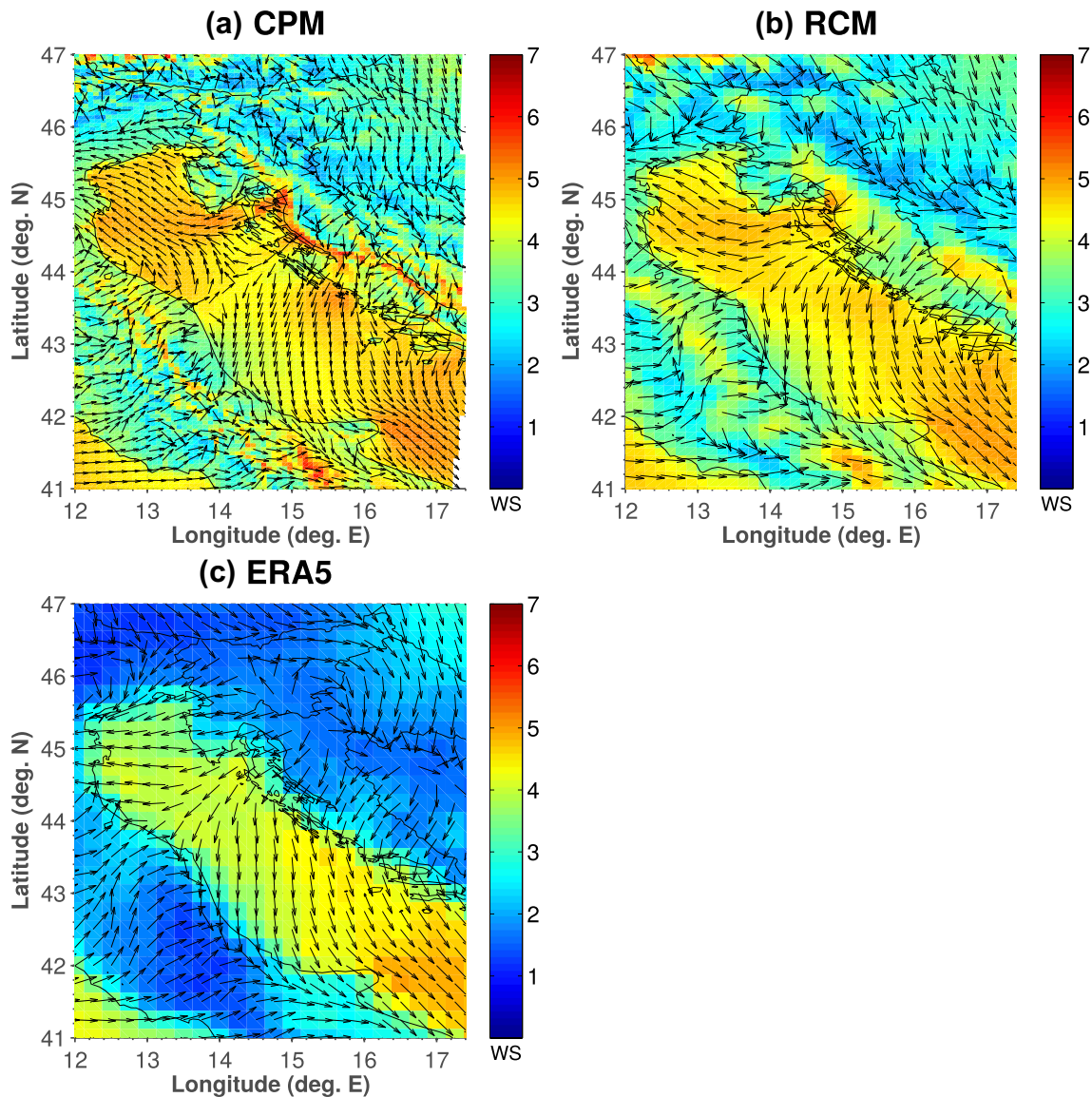


Fig. 3 Same as Fig. 2, but for summer (JJA)

The variability of the wind field over land is largely influenced by fine-scale topography, while the wind field over the open sea (distance more than 80 km from the coast) is mostly affected by large-scale atmospheric circulations (Herrmann et al. 2011; Menendez et al. 2014). Following this, the wind field over the Adriatic region experiences the influence of different types of surfaces. Over the open sea region, which is reliably simulated also by coarse-resolution simulations (Di Luca et al. 2015), and where the wind field is more uniform, all simulations show similar results in both seasons. Over the Croatian lowlands (eastern part of Croatia, Fig. 1), the prevailing wind in RCMs (Figs. 2b and 3b) does not deviate significantly from the relatively weak N-NW wind in ERA5 (Figs. 2c and 3c) in both seasons. Differences are evident in CPMs

(Figs. 2a and 3a) in the vicinity of the isolated mountains in the lowlands.

Regardless of the horizontal grid spacing, the wind direction over the coastal region in the eastern Adriatic is predominantly from the NE. On the other hand, refining the grid spacing is important for the wind speed in the coastal region, where topography plays a significant role in the wind field modifications. Potential added value introduced by CPMs (Figs. 2a and 3a) can be seen in smaller-scale wind structures indicating more variable wind speed and direction. These structures are related to the Bora jets and wakes, where the jets are associated with coastal mountain passes, particularly downstream of the Velebit mountain stretching along the northern Adriatic coastline (Fig. 1), as observed in measurements and case-study simulations (Grisogono and

Belušić 2009; Grubišić 2004; Prtenjak et al. 2015; Stiperski et al. 2012; Večenaj et al. 2012). The maximum wind speed associated with the Bora jet in Fig. 2a is 11 ms^{-1} . On the other hand, these jets are hardly visible in coarser resolution simulations, which have a smaller spread in magnitude (maximum of 8 ms^{-1} within the jet in Fig. 2b and 6.5 ms^{-1} in Fig. 2c).

3.2 Severe wind speeds

The indication of potential added value in terms of the seasonal (DJF, JJA) spatial extremes is addressed here. If considering the whole PDF when calculating the PSS, no clear added value of CPMs is evident. Therefore, we focus only on the strongest winds as explained in Sect. 2.4.

Figure 4 shows the ratio in number of events between CPMs and their parent RCMs, for Q95 larger than 5 ms^{-1}

(Fig. 4a and c) and 15 ms^{-1} (Fig. 4b and d). There are no bars for KNMI and HCLIMcom in Fig. 4d since their RCMs have no values larger than 15 ms^{-1} in JJA. The Q95 larger than 5 ms^{-1} represents 90% of data in all simulations, with almost no differences in the number of events in CPMs and RCMs. Strong wind events ($Q95 > 15 \text{ ms}^{-1}$) are mainly more frequent in CPMs compared to RCMs (on average around 1.3 times more frequent in DJF for 2/3 of CPMs, and 1.5 times more frequent in JJA for almost all CPMs). Those extreme events constitute a relatively small (10% in DJF and $< 1\%$ in JJA) portion of the whole dataset. Due to the very small occurrence of such events in JJA, the potential added value is more important for the cold season.

Here we also show how different statistical indices can result with different potential added value depending on which part of the frequency distribution is sampled. That is, higher percentiles (strong winds) of the distribution show a

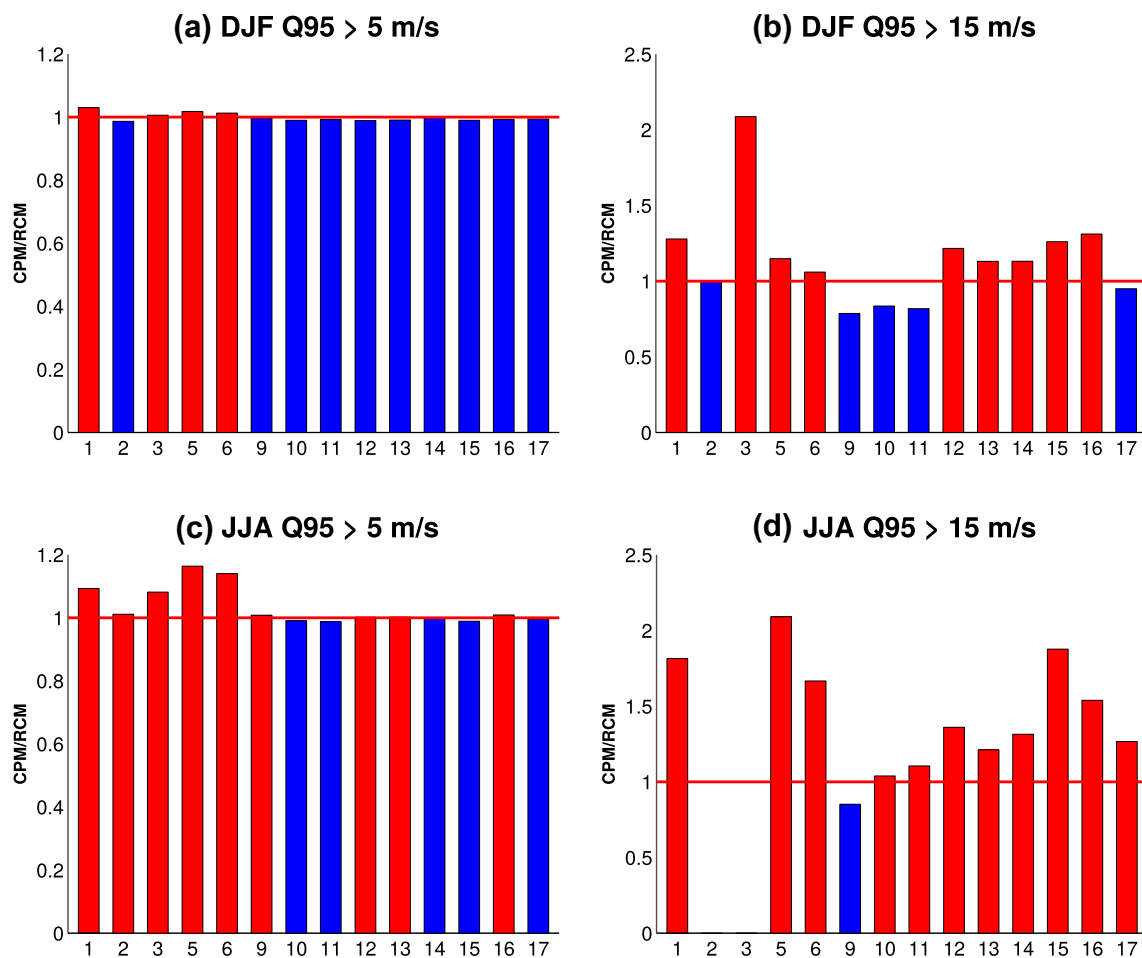


Fig. 4 Ratio of frequency distribution of spatial Q95 (95th percentile) of the wind speed for all available pairs of CPM-RCM simulations. First row (a, b) cold season (DJF), second row (c, d) warm season (JJA). a, c $Q95 > 5 \text{ ms}^{-1}$, b, d $Q95 > 15 \text{ ms}^{-1}$. Red bars indicate CPM v. RCM ratio larger than 1, while blue bars indicate ratio smaller than

1. Numbers in the x-axis correspond to the first column in Table 1. There is no value for groups 2 (KNMI) and 3 (HCLIMcom) in Fig. 4d since their RCMs have no values larger than 15 ms^{-1} in JJA. Groups 4, 7 and 8 are also missing since there are no corresponding RCM data

much larger sensitivity to changes in resolution than central moments (moderate winds). Such a sensitivity of the potential added value to the resolution change is also evident for other variables, such as precipitation (Ban et al. 2021; Ciarlo et al. 2021; Di Luca et al. 2012; Torma et al. 2015).

3.3 Bora and Sirocco

In previous sections, we showed that severe winds, which involve Bora and Sirocco along the Adriatic, could be simulated more reliably by CPMs at the seasonal scale. Here, we compare the simulated wind field to the actual observations over the whole observed period. Since different regimes generate the wind flow in the coastal and the continental part of the Adriatic region, we do not expect CPMs to have the same skill in simulating the wind field over the entire domain. Furthermore, we examine the individual performances of model-based ensembles (AROME ensemble, COSMO ensemble, RegCM and WRF ensemble) in order to examine the differences among CPMs.

Wind rose frequencies (Figs. 5 and 6), as well as entire wind roses (both frequencies and intensities, Fig. 7) from observational stations, CPM ensemble means and the corresponding RCM ensemble means are shown for several station representative of different conditions and regions (Fig. 1: a) Zagreb-Maksimir—inland station, b) Pula airport—coastal station in flat terrain, c) Trieste, d) Senj and e) Split airport—three coastal stations in the complex terrain). Two stations (Zagreb-Maksimir and Pula airport) have more uniform distribution of wind directions, while three stations (Trieste, Senj and Split airport) are in the complex coastal terrain where Bora and Sirocco play a significant role and are the most frequent and intense. Trieste and Senj are Bora representatives (e.g., Grisogono and Belušić 2009; Kuzmić et al. 2013; Prtenjak et al. 2015), while Split airport is a Sirocco representative (e.g., Međugorac et al. 2015; Pasarić et al. 2007).

For the inland station (Zagreb-Maksimir, black line in Figs. 5a and 6a), all wind directions in the observations are mostly equally represented with the maximum wind speed from 67.5° (NE direction) reaching 9.6 ms^{-1} (Fig. 7c). Both CPMs and RCMs tend to overestimate the observed wind speed (Fig. 7a and b). The individual frequency distributions show that RCM (red color in Fig. 6a) ensembles perform well for the NE directions, but there is a southern shift for the most frequent western direction. On the other hand, CPM ensembles for Zagreb-Maksimir are less successful in simulating the NE directions. In the flat coastal part of the Adriatic region (Pula airport) N-NE winds prevail (Fig. 7f) contributing $\sim 48\%$ to the observed frequency distribution (where 25% is within the defined Bora range). The maximum observed wind speed is 17 ms^{-1} blowing from 30°

(Fig. 7f). CPM (Fig. 5b) and RCM (Fig. 6b) ensembles correctly simulate the wind speed distribution for the NE direction, but slightly underestimate the frequencies for the N direction. For these two stations in the flat terrain, dividing the ensemble into model-based smaller ensembles (Figs. 5a, b and 6a, b) did not result in any additional differences and the added value of CPMs is hardly visible here.

Bora dominates over the complex terrain of the northern Adriatic, and is observed very frequently at its jets (Table 2): Trieste (44% of the time in Fig. 7i) and Senj (49% of the time in Fig. 7l) stations. The frequency of occurrence of Bora in the CPM ensemble is 34% at Trieste (Fig. 7g) and 50% at Senj (Fig. 7j), while RCMs have Bora 36% of the time at Trieste (Fig. 7h), and 46% at Senj (Fig. 7k). Furthermore, model-based CPM ensembles (Fig. 5c and d) show that the underestimation of frequency of Bora in Bora jets (Trieste and Senj) is due the contribution of RegCM and WRF in the ensemble (Table 2). AROME (blue) and COSMO (green) ensembles have the best agreement with observations.

The maximum observed 3-h Bora wind speed at Trieste is 20 ms^{-1} blowing from 50° (Fig. 7i), at Senj it is 19 ms^{-1} blowing from 22.5° (Fig. 7l). However, the actual wind speed at Senj should be considerably larger. This issue has previously been addressed by Bencetić Klaić et al. (2009), who show that the location of the Senj observational station is shielded from the Bora directions and therefore underestimates the Bora wind speed. They conclude that the wind speed observed at the station is underestimated by about 40%, but the wind direction is realistic. Thus, the conclusion is that the observed maximum wind speed at Senj would reach 33 ms^{-1} . The maximum wind speed from CPMs is realistic for both Trieste (ensemble mean is 24 ms^{-1} , Fig. 7g), and Senj (ensemble mean is 32 ms^{-1} , Fig. 7j), considering the above-mentioned underestimation of the Bora wind speed for the latter. It is also important to note here that despite the previously mentioned underestimation of the number of Bora events by the WRF ensemble, it reproduces the maximum wind speeds very successfully in Bora jets. RCMs fairly underestimate the maximum wind speed and produce a Bora maximum of 15 ms^{-1} at Trieste station and 27 ms^{-1} at Senj station. Summing up everything that has been stated for the Bora wind, moving to the complex coastal terrain the added value of CPMs becomes more pronounced; while at Trieste CPMs perform better only in terms of the wind speed, the added value of CPMs for both frequency and intensities at Senj is clearly evident.

Further south along the coastline (Split airport), Sirocco plays an important role and becomes more comparable to Bora (18%, Table 2) in the number of observed events (Fig. 7o), with Sirocco occurring 13% of the time (Table 3). However, the maximum wind speed still occurs for the Bora wind (Fig. 7o). The representation of both Sirocco maximum wind speed (ensemble mean is 15 ms^{-1} ,

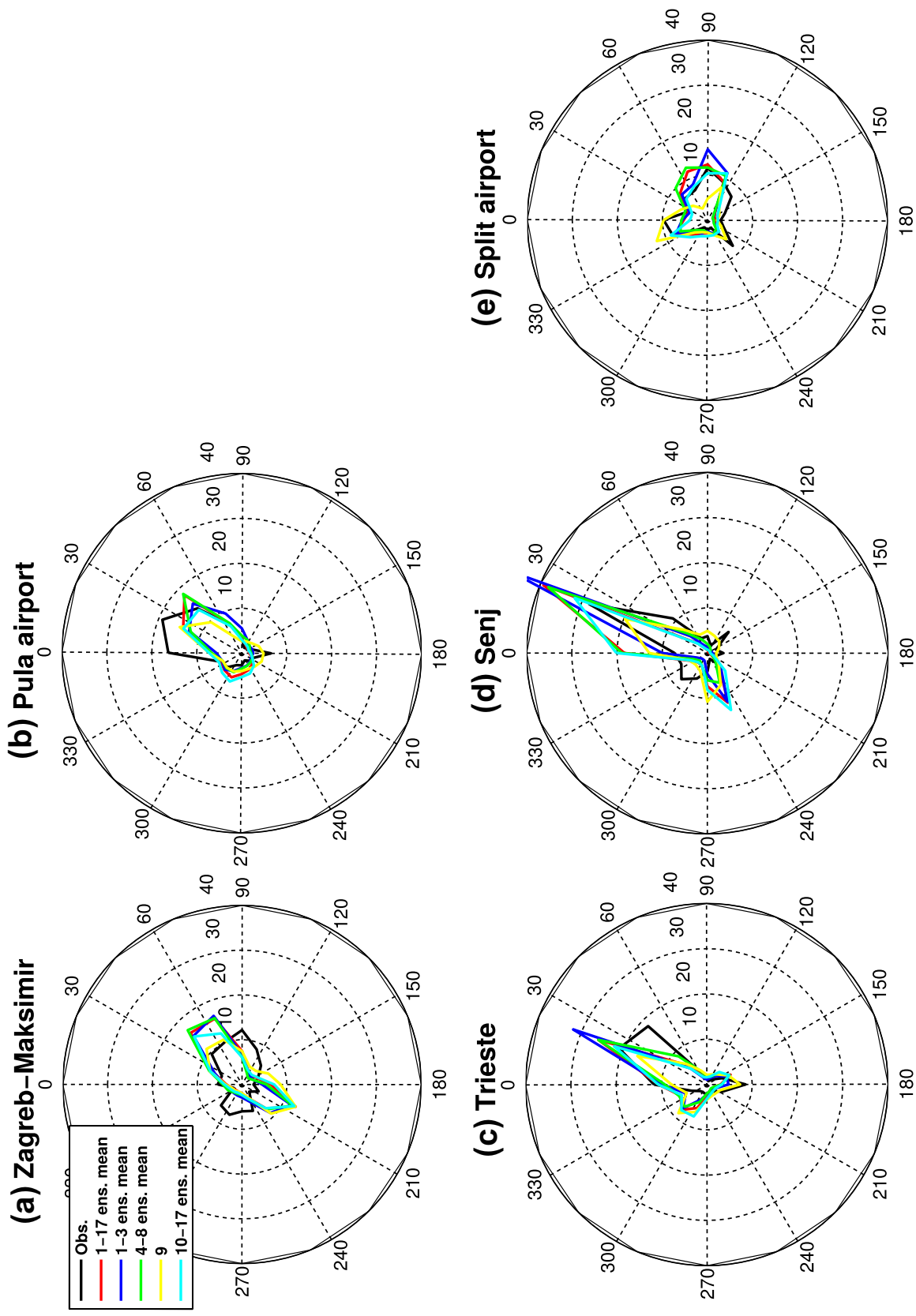


Fig. 5 Wind roses (frequencies in %) obtained from CPMs for stations indicated in Fig. 1 over the whole analyzed period: **a** Zagreb-Maksimir, **b** Pula airport, **c** Trieste, **d** Senj and **e** Split airport. Observations are in black, the whole CPM (1–17) ensemble mean in red, AROME (1–3) ensemble mean in blue, CCLM (4–8) ensemble mean in green, RegCM (9) in yellow and WRF (10–17) ensemble mean in cyan

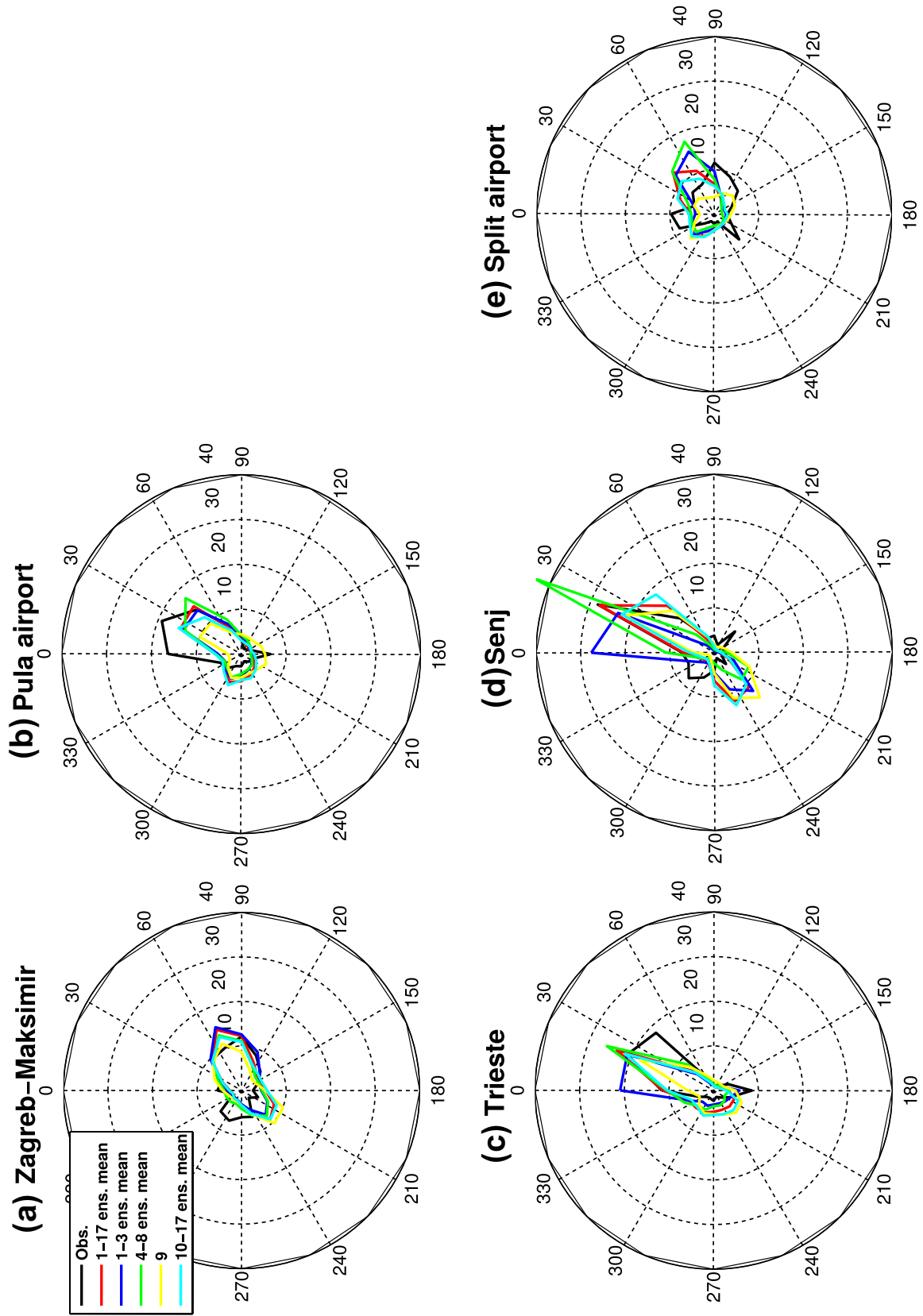


Fig. 6 Same as Fig. 5, but for RCMs

Table 2 Bora (22–68.5°) number of events and maximum wind speed at Trieste, Senj and Split airport obtained from CPM ensemble mean, RCM ensemble mean and observations

	Number of events	CPM ensemble mean	RCM ensemble mean	Observations
	Maximum wind speed	AROME ensemble mean	AROME ensemble mean	
		COSMO ensemble mean	COSMO ensemble mean	
		RegCM	RegCM	
		WRF ensemble mean	WRF ensemble mean	
Trieste		9979 (34%) 24 ms ⁻¹	10,372 (36%) 15 ms ⁻¹	12,730 (44%) 20 ms ⁻¹
		12,092 (41%) 19 ms ⁻¹	10,968 (38%) 15 ms ⁻¹	
		10,491 (36%) 21 ms ⁻¹	11,948 (41%) 15 ms ⁻¹	
		8817 (30%) 23 ms ⁻¹	9121 (31%) 14 ms ⁻¹	
		9012 (31%) 29 ms ⁻¹	9912 (34%) 16 ms ⁻¹	
Senj		14,496 (50%) 32 ms ⁻¹	13,442 (46%) 27 ms ⁻¹	14,293 (49%) 19 ms ⁻¹
		16,621 (57%) 28 ms ⁻¹	14,363 (50%) 18 ms ⁻¹	
		15,409 (53%) 28 ms ⁻¹	16,728 (57%) 16 ms ⁻¹	
		11,290 (39%) 27 ms ⁻¹	11,872 (41%) 28 ms ⁻¹	
		13,530 (46%) 37 ms ⁻¹	12,471 (43%) 33 ms ⁻¹	
Split airport		5697 (20%) 19 ms ⁻¹	7657 (26%) 17 ms ⁻¹	5349 (18%) 23 ms ⁻¹
		5706 (20%) 19 ms ⁻¹	7570 (26%) 12 ms ⁻¹	
		7601 (26%) 20 ms ⁻¹	9873 (34%) 17 ms ⁻¹	
		5728 (20%) 21 ms ⁻¹	6153 (21%) 21 ms ⁻¹	
		4501 (15%) 19 ms ⁻¹	7323 (25%) 18 ms ⁻¹	

Table corresponding to Figs. 5, 6, and 7

Table 3 As Table 2, but for Sirocco (112.5–157.5°)

	Number of events	CPM ensemble mean	RCM ensemble mean	Observations
	Maximum wind speed	AROME ensemble mean	AROME ensemble mean	
		COSMO ensemble mean	COSMO ensemble mean	
		RegCM	RegCM	
		WRF ensemble mean	WRF ensemble mean	
Trieste		2463 (8%) 15 ms ⁻¹	884 (3%) 17 ms ⁻¹	934 (3%) 15 ms ⁻¹
		1877 (6%) 14 ms ⁻¹	917 (3%) 18 ms ⁻¹	
		2467 (8%) 13 ms ⁻¹	1056 (4%) 17 ms ⁻¹	
		1877 (6%) 16 ms ⁻¹	1237 (4%) 19 ms ⁻¹	
		2475 (9%) 16 ms ⁻¹	785 (3%) 17 ms ⁻¹	
Senj		1255 (4%) 13 ms ⁻¹	690 (2%) 10 ms ⁻¹	3009 (10%) 16 ms ⁻¹
		1042 (4%) 19 ms ⁻¹	341 (1%) 16 ms ⁻¹	
		1537 (5%) 12 ms ⁻¹	485 (2%) 16 ms ⁻¹	
		2105 (7%) 12 ms ⁻¹	1008 (3%) 15 ms ⁻¹	
		1052 (4%) 15 ms ⁻¹	831 (3%) 13 ms ⁻¹	
Split airport		3207 (11%) 15 ms ⁻¹	2352 (8%) 12 ms ⁻¹	3649 (13%) 13 ms ⁻¹
		2133 (7%) 14 ms ⁻¹	1962 (7%) 19 ms ⁻¹	
		3017 (10%) 13 ms ⁻¹	1687 (6%) 12 ms ⁻¹	
		2676 (9%) 14 ms ⁻¹	3445 (12%) 15 ms ⁻¹	
		3794 (13%) 16 ms ⁻¹	2528 (9%) 13 ms ⁻¹	

while 13 ms⁻¹ is observed, Table 3) and frequency (11%, Fig. 5e and Table 3) is realistic with CPMs. In contrast, the skill of RCMs in simulating the wind speed and direction reduces moving southward (Table 3). RCMs cannot be taken as representative due to their inability to simulate Sirocco events from the defined angle range (8%, Fig. 6e and Table 3). They tend to simulate an exaggerated number (Table 2, 26% of Bora events compared to the observed 18%) of moderate (maximum of 17 ms⁻¹ simulated, while 23 ms⁻¹ is observed) Bora events at Split airport, as well as along the whole southern Adriatic. Hence, CPMs provide a

clear added value compared to RCMs regarding the Sirocco frequency. Accordingly, all these points disclose directly the link between better resolved topography and the representation of the wind. Sirocco events in the southern Adriatic were also poorly simulated by the previously examined CORDEX RCM simulations with daily time step (Belušić et al. 2018). Subdividing the CPM ensembles for Sirocco, we noted smaller differences between respective ensembles than for Bora (Fig. 5).

Extracting only the direction ranges defined for Bora and Sirocco and focusing on the cold season (DJF) we can

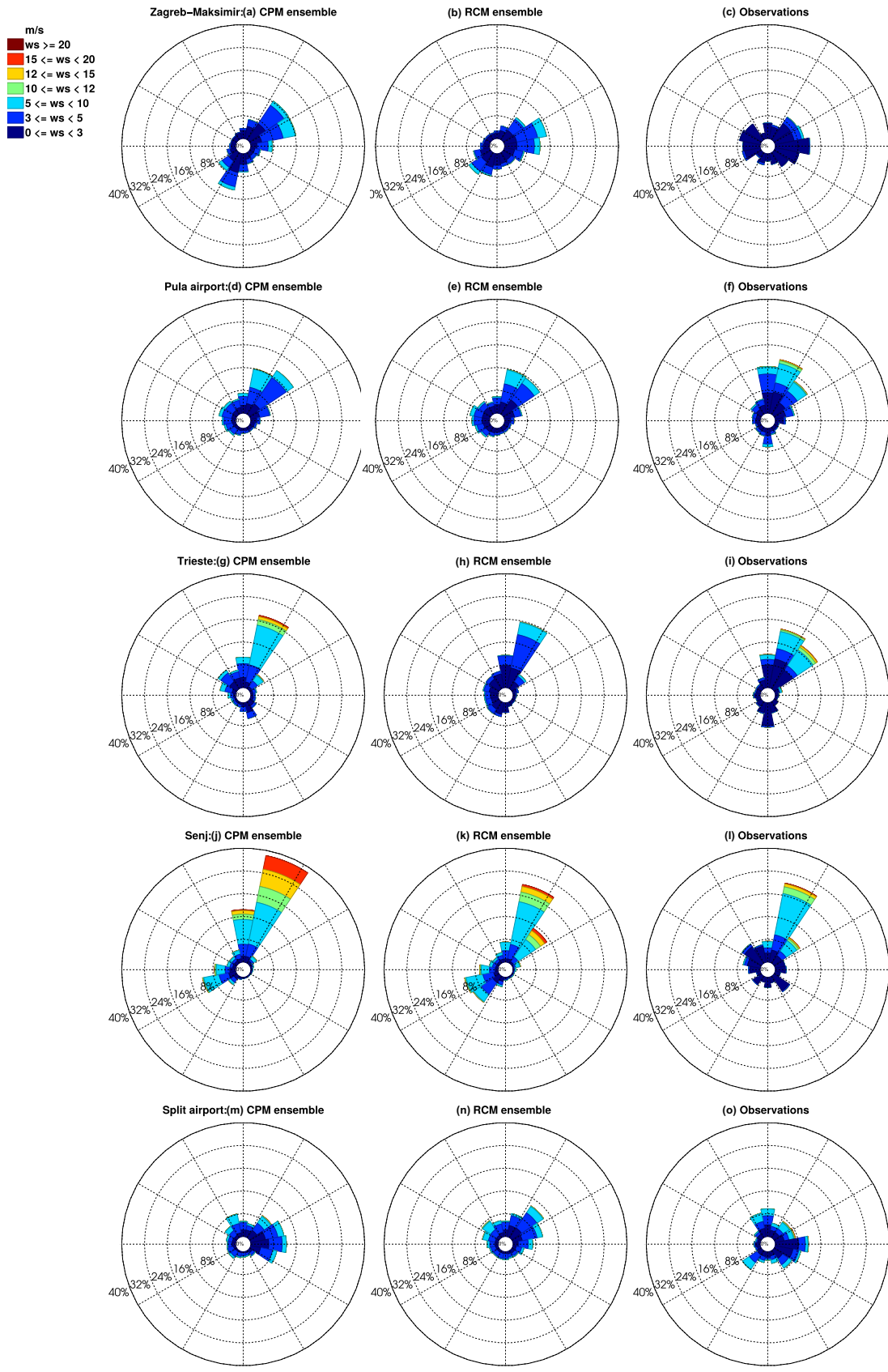


Fig. 7 Wind roses for stations indicated in Fig. 1 over the whole analyzed period: Zagreb-Maksimir (first row), Pula airport (second row), Trieste (third row), Senj (fourth row) and Split airport (fifth row). CPM ensemble mean (first column), RCM ensemble mean (second column) and observations (third column). Colors indicate wind speed

inspect the added value in more detail. Figure 8 shows the DJF Bora maximum wind speeds at Trieste and Sirocco frequencies of occurrence at Split airport. Benefits introduced by CPMs are especially evident for these parameters and are hence in focus here. The maximum observed wind speed of the DJF Bora events at Trieste is 20 ms^{-1} and is simulated by CPMs very well (COSMO simulations, numbers 4–8 in Fig. 8a, have the best skill), except for the WRF simulations (numbers 10–17), which overestimate the maximum by 20%. On the other hand, RCMs and ERA5 perform similarly and underestimate the maximum wind speed by $\sim 30\%$.

Sirocco frequencies, defined as strictly along shore in the southern Adriatic, are poorly simulated by RCMs, but CPMs approach the observations. The underestimation of the observed number of Sirocco events by RCMs and ERA5 is $\sim 50\%$, and is larger compared to Bora (20%). Figure 8b supports the fact that CPMs strongly enhance the number of Sirocco events for almost all the simulations analyzed. The simulated frequencies come very close to the observations (~ 1000 events in DJF) except for simulations 1–3 (AROME model). These simulations would perform better for Sirocco angle definition starting at $\sim 105^\circ$, while our Sirocco definition takes into account wind direction starting from 112.5° . In contrast to the Bora events, the WRF ensemble (numbers 10–17) for Sirocco shows the best performance.

3.4 The skill in basic temporal statistical measures

Standard temporal statistical measures for all available simulations and for all analyzed stations are shown in Fig. 9. We can notice immediately that each CPM is strongly influenced by its parent RCM. If the RCM does not perform well, there are low chances that the child CPM will. This implies, for the used statistical measures, that the choice of resolution (CPM or RCM) affects the final results much less than the choice of the particular modeling system. Therefore, there is no clear added value of CPMs for the standard temporal statistical scores. This was also true when comparing the coarse (50 km) and fine (12 km) resolution RCMs in Belušić et al. (2018).

The difference between the inland and coastal regions is in the larger spread among the stations for the latter for a particular statistical parameter. Grouping all the available stations for each terrain type (Fig. 9), the general picture is as follows. Most of the biases over the inland stations are close to zero or positive, in the range of $1\text{--}2 \text{ ms}^{-1}$ (Fig. 9a), indicating a slight wind speed overestimation in the simulations as was already indicated in Sect. 3.3. Furthermore, the maximum biases in the coastal region with the complex terrain are two times larger than those for other regions, ranging from 1 to 4 ms^{-1} , indicating also a large spread of biases among coastal stations. The simulated standard deviation for inland stations (Fig. 9a) usually follows the observed one very well, while in the complex terrain (Fig. 9b), where the wind intensity is high, the simulated standard deviation is up to 6 times larger than the observed one (depending on the simulation and station chosen). Summarizing, higher moments (i.e., standard deviation) of the distribution are

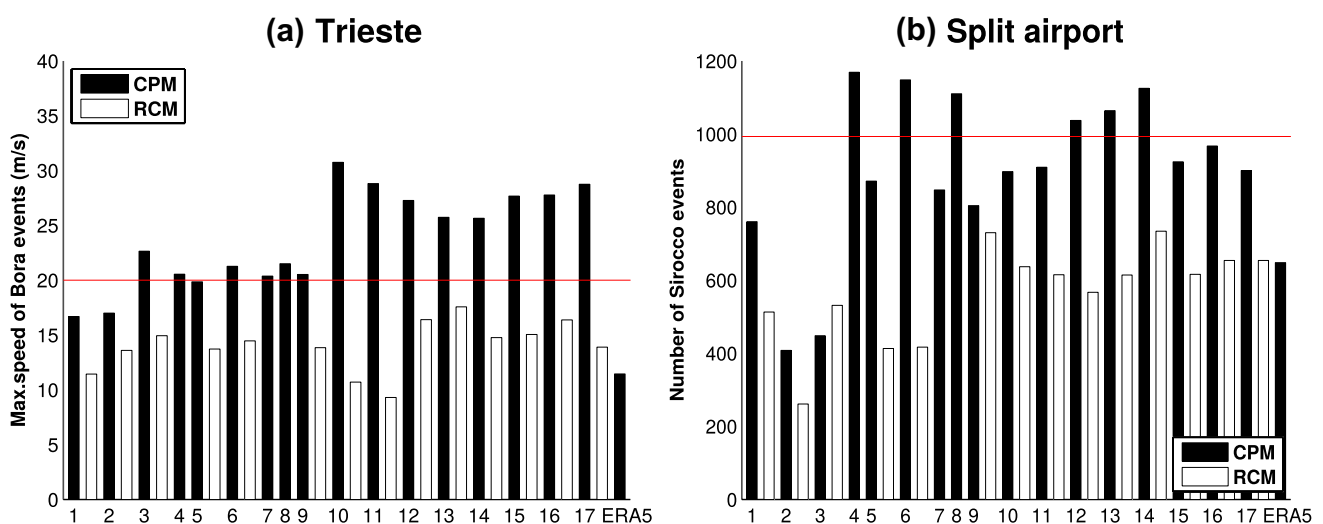


Fig. 8 Cold season (DJF) Bora ($22.5\text{--}68.5^\circ$) maximum wind speed at Trieste (a) and Sirocco ($112.5\text{--}157.5^\circ$) frequencies at Split airport (b) from all available simulations. Red line represents the observed values

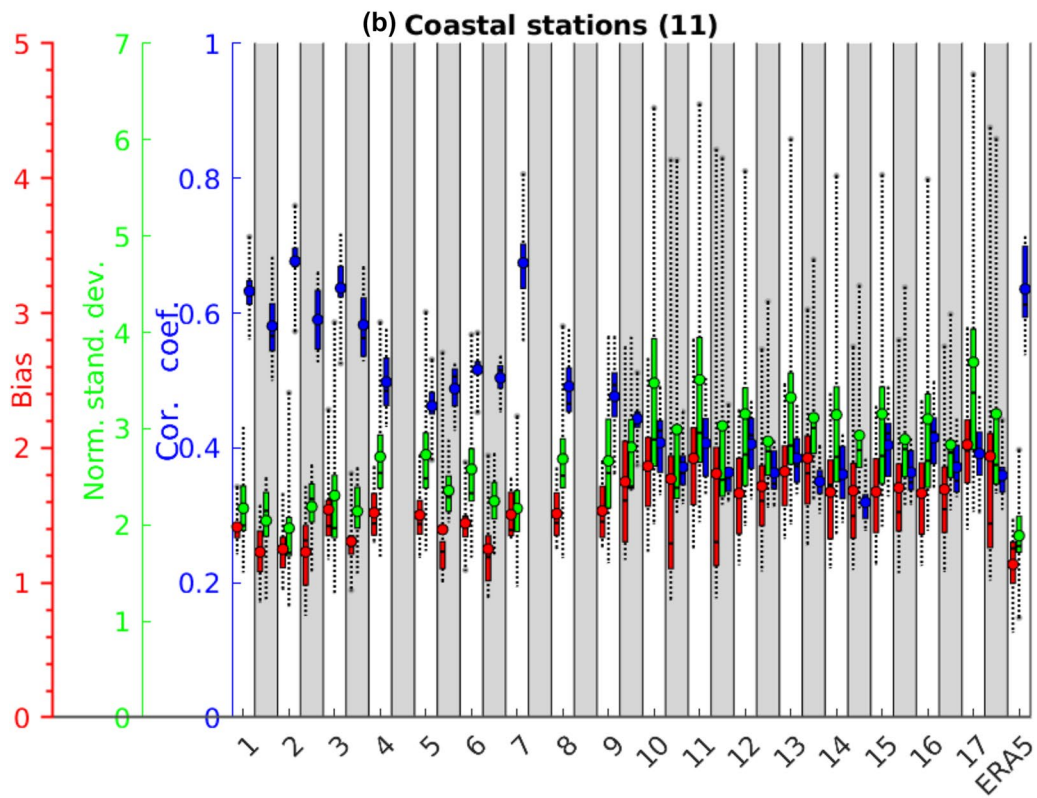
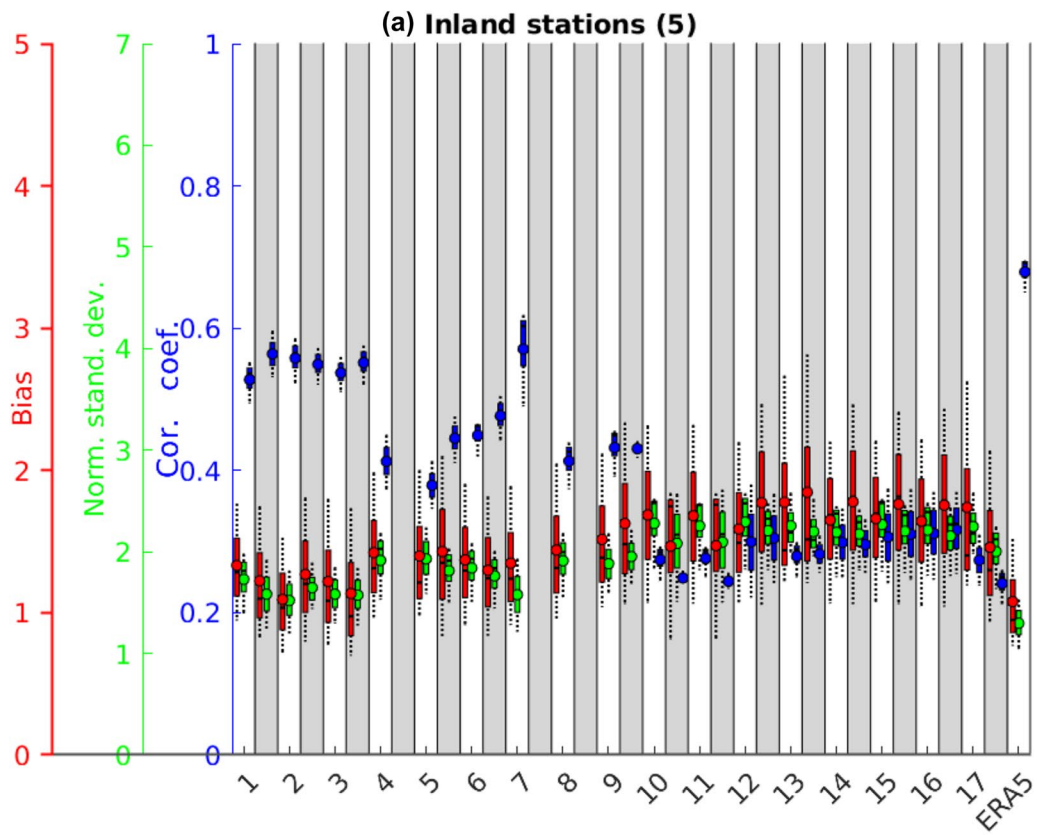


Fig. 9 Standard statistical measures for all available simulations and for all analyzed stations. Three sets of values correspond to each simulation from 1 to ERA5 (bias in red, normalized standard deviation in green and correlation coefficient in blue), while each box-plot contains the values from all the stations in the group (5 inland stations and 11 coastal stations). Numbers on the x-axis indicate correspond to the first column in Table 1. CPM values are in white boxes, while the corresponding RCMs are shaded in gray (gray boxes for CPMs without a corresponding RCM are left blank). The last group of values is for ERA5

not simulated as well as the central moments (i.e., mean) for both CPMs and RCMs. The present comparison between inland and coastal stations agrees with Belušić et al. (2018) and Obermann et al. (2016). However, the exact values should be interpreted with caution, since the in-situ observations are not necessarily entirely representative for the gridded climate model output.

Even if climate simulations with CPMs and RCMs are not primarily designed to exactly follow the development of weather events, some members from the analyzed ensemble manage to follow the observed time series very accurately regardless of the internal variability inside the domain (AROME model, numbers 1 to 3 from Table 1). As expected, the ERA5 reanalysis (last blue value in Fig. 9) usually has the largest temporal correlation coefficient at all analyzed stations, since a large amount of observational data is assimilated, but it has lower standard deviation due to the resolution limitations.

The dispersion of scores among CPMs are as follows. The CPM simulations from 1 to 3 (AROME), and consequently their parent RCM simulations, appear to best fit the observations at all available stations, having the smallest biases, being the closest to the observed standard deviation, and having the greatest temporal correlation coefficient (very close to the one obtained from ERA5). On the other hand, the simulations between lines 10 and 17 (WRF) have larger spread in biases, quite large normalized standard deviation for coastal stations and considerably lower temporal correlation coefficients for both inland and coastal stations.

4 Summary and conclusions

The main goal of this study was to assess the (potential) added value obtained by downscaling RCMs with CPMs in terms of the wind field over the Adriatic domain. We used 3-h wind data obtained from the CORDEX-FPS on convection ensemble, consisting of 17 CPMs and 14 RCMs in the period 2000–2009. We show where and with respect to which climate statistics the CPMs can produce more skillful results than the RCMs. Furthermore, we examine differences between individual CPMs in order to see if strong differences exist. In general, results confirm the benefits of

using high-resolution CPMs and the conclusions based on the four points proposed in the introduction are as follows:

- *The enhanced spatial variability.*

CPMs display small-scale spatial variability that is absent in coarser RCMs or reanalysis, leading to a larger spread in intensities which allows for capturing more extreme events. They are especially evident along the mountainous ranges in the coastal part of the Adriatic region and in the vicinity of the isolated mountains in the lowlands. This is highly important for the realistic simulation of severe wind formations such as Bora jets.

- *The possibility of simulating more intense wind speeds.*

Severe wind events are mostly associated with the Bora wind in the cold season. Therefore, the potential added value of CPMs is higher in the cold season compared to the warm season because of the larger proportion of severe wind events. Severe winds are more frequent in CPMs and can be more realistically simulated by them. Furthermore, the results indicate that intense wind events have considerably larger sensitivity to the changes in resolution than low to moderate wind speed events.

- *Having enough skill to replicate the observed wind roses over the complex terrain and the ability to simulate local winds realistically.*

Both the CPMs and RCMs generally perform well in the flat terrain. In regions with complex topography, the orographic forcing emphasizes the added value of CPMs: the RCMs lose the skill in simulating both the wind speed and direction distributions compared to the flat-terrain results, while the CPMs keep the reliable results. The main benefit of using CPMs is detected for the Bora maximum wind speeds in the northern Adriatic and for the Sirocco frequencies in the southern Adriatic. This discloses directly the link between the better resolved topography and the representation of the wind.

- *The skill in producing temporal correlation coefficient as high as in ERA5.*

Even if climate simulations with CPMs and RCMs are not envisaged to exactly follow the development of observed weather events, the assessment of the correlation coefficient showed that some of them manage to reproduce the observed time series well. We noticed that the choice of resolution (CPM or RCM) affects the statistical results much less than the choice of the particular CPM.

Acknowledgements All authors gratefully acknowledge the WCRP-CORDEX-FPS on Convective phenomena at high resolution over Europe and the Mediterranean (FPSCONVALP- 3) and the research data exchange infrastructure and services provided by the Jülich Supercomputing Centre, Germany, as part of the Helmholtz Data Federation initiative. The ETH, IPSL, ICTP, SMHI, CMCC, KNMI acknowledge funding from the HORIZON 2020 EUCP (European Climate Prediction System) project (<https://www.eucp-project.eu>, grant agreement No. 776613). IPSL's work was granted access to the HPC resources of TGCC under the allocations 2019-A0030106877 and 2020-A0030106877 made by GENCI. DB acknowledges funding from the FORMAS project EDUCAS (grant no. 2019-00829). MED acknowledges the Partnership for advanced computing in Europe (PRACE) for awarding access to Piz Daint at ETH Zürich at the Swiss National Supercomputing Centre (CSCS, Switzerland). MED also acknowledges the Federal Office for Meteorology and Climatology (MeteoSwiss), CSCS, the Center for Climate Systems Modeling (C2SM) and ETH Zürich for their contributions to the development and maintenance of the GPU-accelerated version of COSMO. ØH has received support from the project GREAT, funded by the Research Council of Norway (grant no. 275589), and acknowledge computing resources from Notur (NN9188K). SK acknowledges the support of the Greek Research and Technology Network (GRNET) High Performance Computing (HPC) infrastructure for providing the computational resources of AUTH-simulations (under project IDs pr003005 and pr009020) and the AUTH Scientific Computing Center for technical support. JM acknowledges the support from the Spanish Agencia Estatal de Investigación through the Unidad de Excelencia María de Maeztu with reference MDM-2017-0765, the projects CORDyS (PID2020-116595RB-I00) and ATLAS (PID2019-111481RB-I00), both funded by MCIN/AEI/10.13039/501100011033. EP acknowledges the Consorzio Inter-universitario per il Calcolo Automatico dell'Italia Nord Orientale (CINECA) super-computing center (Bologna, Italy) for computing resources dedicated to ICTP simulations. HT is thankful for the computational resources granted by the John von Neumann Institute for Computing (NIC) and provided on the supercomputer JURECA at the Jülich Supercomputing Centre (JSC) through the grant JJSC39 and for the computational resources at the Vienna Scientific Cluster (VSC) through the grants 70992 and 71193, the long-term storage provided by the cooperation project GEOCLIM Data Infrastructure Austria, funded by the Austrian Education, Science and Research Ministry (BMBWF), as well as for the support received via the project "reclip:convex", funded by the Austrian Climate Research Programme (ACRP) of the Klima- und Energiefonds (no. B769999).

Author contributions ABV, DB, MTP and IG contributed to the study conception and design. Material preparation, data collection and analysis were performed by ABV. The authors DB and from SB to KWS performed the simulations. The first draft of the manuscript was written by ABV and all authors commented on previous versions of the manuscript. All authors read and approved the final manuscript.

Funding The ETH, IPSL, ICTP, SMHI, CMCC, KNMI was supported by the HORIZON 2020 EUCP (European Climate Prediction System) project (<https://www.eucp-project.eu>, grant agreement No. 776613). DB was supported by the FORMAS project EDUCAS (grant no. 2019-00829). HT was supported by the John von Neumann Institute for Computing (NIC) through the grant JJSC39 and by Vienna Scientific Cluster (VSC) through the grants 70992 and 71193, the long-term storage provided by the cooperation project GEOCLIM Data Infrastructure Austria, funded by the Austrian Education, Science and Research Ministry (BMBWF). HT was supported via the project "reclip:convex", funded by the Austrian Climate Research Programme (ACRP) of the Klima- und Energiefonds (no. B769999). JM was supported from the Spanish Agencia Estatal de Investigación through the Unidad de Excelencia María de Maeztu with reference

MDM-2017-0765, the projects CORDyS (PID2020-116595RB-I00) and ATLAS (PID2019-111481RB-I00), both funded by MCIN/AEI/10.13039/501100011033. ØH has received support from the project GREAT, funded by the Research Council of Norway (grant no. 275589).

Data availability The datasets analyzed during the current study are available via the data exchange infrastructure and services provided by the Jülich Supercomputing Centre, Germany, as part of the Helmholtz Data Federation initiative.

Declarations

Conflict of interest The authors have no relevant financial or non-financial interests to disclose.

References

- Adinolfi M, Raffa M, Reder A, Mercogliano P (2021) Evaluation and expected changes of summer precipitation at convection permitting scale with COSMO-CLM over alpine space. *Atmosphere* 12(1):54. <https://doi.org/10.3390/atmos12010054>
- Bajić A (1989) Severe bora on the northern Adriatic part I: statistical analysis. *Croatian Meteorol J* 24(24):1–9
- Baldauf M, Seifert A, Förstner J, Majewski D, Raschendorfer M, Reinhardt T (2011) Operational convection-scale numerical weather prediction with the COSMO model: description and sensitivities. *Mon Weather Rev* 139:3887–3905. <https://doi.org/10.1175/MWR-D-10-05013.1>
- Ban N, Schmidli J, Schär C (2014) Evaluation of the convection-resolving regional climate modeling approach in decade-long simulations. *J Geophys Res Atmos* 119:7889–7907. <https://doi.org/10.1002/2014JD021478>
- Ban N, Schmidli J, Schär C (2015) Heavy precipitation in a changing climate: does short-term summer precipitation increase faster? *Geophys Res Lett* 42:1165–1172. <https://doi.org/10.1002/2014GL062588>
- Ban N, Caillaud C, Coppola E et al (2021) The first multi-model ensemble of regional climate simulations at kilometer-scale resolution, part I: evaluation of precipitation. *Clim Dyn* 57:275–302. <https://doi.org/10.1007/s00382-021-05708-w>
- Belušić A, Prtenjak MT, Güttler I, Ban N, Leutwyler D, Schär C (2018) Near-surface wind variability over the broader Adriatic region: insights from an ensemble of regional climate models. *Clim Dyn* 50:4455–4480. <https://doi.org/10.1007/s00382-017-3885-5>
- Belušić D, de Vries H, Dobler A et al (2020) HCLIM38: a flexible regional climate model applicable for different climate zones from coarse to convection permitting scales. *Geosci Model Dev* 13:1311–1333. <https://doi.org/10.5194/gmd-13-1311-2020>
- Belušić Vozila A, Güttler I, Ahrens B, Obermann-Hellhund A, Telišman Prtenjak M (2019) Wind over the Adriatic region in CORDEX climate change scenarios. *J Geophys Res Atmos* 124:110–130. <https://doi.org/10.1029/2018JD028552>
- Belušić Vozila A, Telišman Prtenjak M, Güttler I (2021) A weather-type classification and its application to near-surface wind climate change projections over the Adriatic Region. *Atmosphere* 12(8):948. <https://doi.org/10.3390/atmos1208094>
- Benčić Klaić Z, Prodanov AD, Belušić D (2009) Wind measurements in Senj – underestimation of true bora flows. *Geofizika* 26(2):245–252
- Bonaldo D, Bucchignani E, Ricchi A, Carniel S (2017) Wind storminess in the Adriatic Sea in a climate change scenario. *Acta Adriat* 58(2):195–208


- Ciarlò JM, Coppola E, Fantini A et al (2021) A new spatially distributed added value index for regional climate models: the EURO-CORDEX and the CORDEX-CORE highest resolution ensembles. *Clim Dyn* 57:1403–1424. <https://doi.org/10.1007/s00382-020-05400-5>
- Colin J, Déqué M, Radu R, Somot S (2010) Sensitivity study of heavy precipitations in Limited Area Model climate simulation: influence of the size of the domain and the use of the spectral nudging technique. *Tellus A* 62:591–604. <https://doi.org/10.1111/j.1600-0870.2010.00467.x>
- Coppola E, Sobolowski S, Pichelli E et al (2020) A first-of-its-kind multi-model convection permitting ensemble for investigating convective phenomena over Europe and the Mediterranean. *Clim Dyn* 55:3–34. <https://doi.org/10.1007/s00382-018-4521-8>
- Coppola E, Stocchi P, Pichelli E, Torres Alavez JA, Glazer R, Giuliani G, Di Sante F, Nogherotto R, Giorgi F (2021) Non-Hydrostatic RegCM4 (RegCM4-NH): model description and case studies over multiple domains. *Geosci Model Dev* 14:7705–7723. <https://doi.org/10.5194/gmd-14-7705-2021>
- Dee DP, Uppala SM, Simmons AJ et al (2011) The ERA-Interim reanalysis: configuration and performance of the data assimilation system. *Q J R Meteorol Soc* 137:553–597. <https://doi.org/10.1002/qj.828>
- Di Luca A, de Elía R, Laprise R (2012) Potential for added value in precipitation simulated by high-resolution nested Regional Climate Models and observations. *Clim Dyn* 38:1229–1247. <https://doi.org/10.1007/s00382-011-1068-3>
- Di Luca A, De Elía R, Laprise R (2015) Challenges in the Queste for added value of regional climate dynamical downscaling. *Curr Clim Change Rep* 1:10–21. <https://doi.org/10.1007/s40641-015-0003-9>
- Fumière Q, Déqué M, Nuissier O, Somot S, Alias A, Caillaud C, Laurantin O, Seity Y (2020) Extreme rainfall in Mediterranean France during the fall: added value of the CNRM-AROME convection-permitting regional climate model. *Clim Dyn* 55:77–91. <https://doi.org/10.1007/s00382-019-04898-8>
- Giorgi F, Coppola E, Solmon F et al (2012) RegCM4: model description and preliminary tests over multiple CORDEX domains. *Clim Res* 52:7–29. <https://doi.org/10.3354/cr01018>
- Grisogono B, Belušić D (2009) A review of recent advances in understanding the meso- and microscale properties of the severe Bora wind. *Tellus A* 61:1–16. <https://doi.org/10.1111/j.1600-0870.2008.00369.x>
- Grubišić V (2004) Bora-driven potential vorticity banners over the Adriatic. *Q J R Meteorol Soc* 130:2571–2603. <https://doi.org/10.1256/qj.03.71>
- Gutowski WJ Jr, Ullrich PA, Hall A et al (2020) The ongoing need for high-resolution regional climate models: process understanding and stakeholder information. *B Am Meteorol Soc* 101(5):E664–E683. <https://doi.org/10.1175/BAMS-D-19-0113.1>
- Herrmann M, Somot S, Calmanti S, Dubois C, Sevault F (2011) Representation of spatial and temporal variability of daily wind speed and of intense wind events over the Mediterranean Sea using dynamical downscaling: impact of the regional climate model configuration. *Nat Hazards Earth Sys Sci* 11:1983–2001. <https://doi.org/10.5194/nhess-11-1983-2011>
- Hersbach H, Bell B, Berrisford P et al (2020) The ERA5 Global Reanalysis. *Q J R Meteorol Soc* 146:1999–2049. <https://doi.org/10.1002/qj.3803>
- Horvath K, Lin YL, Ivančan-Picek B (2008) Classification of cyclone tracks over the Apennines and the Adriatic Sea. *Mon Wea Rev* 136:2210–2227. <https://doi.org/10.1175/2007MWR2231.1>
- Horvath K, Bajjić A, Ivatek-Šahdan S (2011) Dynamical Downscaling of wind speed in complex terrain prone to bora-type flows. *J Appl Meteorol Clim* 50:1676–1691. <https://doi.org/10.1175/2011JAMC2638.1>
- Jacob D, Teichmann C, Sobolowski S et al (2020) Regional climate downscaling over Europe: perspectives from the EURO-CORDEX community. *Reg Environ Change* 20:51. <https://doi.org/10.1007/s10113-020-01606-9>
- Kendon EJ, Prein AF, Senior CA, Stirling A (2021) Challenges and outlook for convection-permitting climate modelling. *Phil Trans R Soc* 379:20190547. <https://doi.org/10.1098/rsta.2019.0547>
- Kuzmić M, Li XM, Grisogono B, Tomažić I, Lehner S (2013) Terra SAR-X observations of the northeastern Adriatic bora: early results. *Acta Adriat* 54:13–26
- Leutwyler D, Lüthi D, Ban N, Fuhrer O, Schär C (2017) Evaluation of the convection-resolving climate modeling approach on continental scales. *J Geophys Res Atmos* 122:5237–5258. <https://doi.org/10.1002/2016JD026013>
- Međugorac I, Pasarić M, Orlić M (2015) Severe flooding along the eastern Adriatic coast: the case of 1 December 2008. *Ocean Dyn* 65(6):817–830. <https://doi.org/10.1007/s10236-015-0835-9>
- Menendez M, García-Díez M, Fita L, Fernández J, Méndez FJ, Gutiérrez JM (2014) High-resolution sea wind hindcasts over the Mediterranean area. *Clim Dyn* 42:1857–1872. <https://doi.org/10.1007/s00382-013-1912-8>
- Meredith EP, Ulbrich U, Rust HW (2020) Subhourly rainfall in a convection-permitting model. *Environ Res Lett* 15:034031. <https://doi.org/10.1088/1748-9326/ab6787>
- Obermann A, Bastin S, Belamari S, Conte D, Gaertner MA, Li L, Ahrens B (2016) Mistral and Tramontane wind speed and wind direction patterns in regional climate simulation. *Clim Dyn* 47:1–18. <https://doi.org/10.1007/s00382-016-3053-3>
- Pasarić Z, Belušić D, Klaić ZB (2007) Orographic influences on the Adriatic sirocco wind. *Ann Geophys* 25:1263–1267. <https://doi.org/10.5194/angeo-25-1263-2007>
- Penzar B, Penzar B, Orlić M (2001) Weather and climate of the Croatian Adriatic (in Croatian). Nakladna kuća “Dr. Feletar”. Zagreb: Hrvatski hidrografski institut
- Perkins SE, Pitman AJ, Holbrook NJ, McAneney J (2007) Evaluation of the AR4 climate models’ simulated daily maximum temperature, minimum temperature, and precipitation over Australia using probability density functions. *J Clim* 20:4356–4376. <https://doi.org/10.1175/JCLI4253.1>
- Pichelli E, Coppola E, Sobolowski S et al (2021) The first multi-model ensemble of regional climate simulations at kilometer-scale resolution part 2: historical and future simulations of precipitation. *Clim Dyn* 56:3581–3602. <https://doi.org/10.1007/s00382-021-05657-4>
- Poje D (1992) Wind persistence in Croatia. *Int J Climatol* 12:569–586. <https://doi.org/10.1002/joc.3370120604>
- Powers JG, Klemp JB, Skamarock WC et al (2017) The weather research and forecasting model: overview, system efforts, and future directions. *B Am Meteorol Soc* 98(8):1717–1737. <https://doi.org/10.1175/BAMS-D-15-00308.1>
- Prtenjak MT, Horvat I, Tomažić I, Kvakić M, Viher M, Grisogono B (2015) Impact of mesoscale meteorological processes on anomalous radar propagation conditions over the northern Adriatic area. *J Geophys Res Atmos* 120:8759–8782. <https://doi.org/10.1002/2014JD022626>
- Rockel B, Will A, Hense A (2008) The regional climate model COSMO-CLM (CCLM). *Meteorol Z* 17:347–348. <https://doi.org/10.1127/0941-2948/2008/0309>
- Ruti PM, Somot S, Giorgi F et al (2016) Med-CORDEX initiative for Mediterranean climate studies. *B Am Meteorol Soc* 97:1187–1208. <https://doi.org/10.1175/BAMS-D-14-00176.1>
- Schär C, Fuhrer O, Arteaga A, Ban N, Charpiilloz C, Di Girolamo S, Hentgen L, Hoefler T, Lapillonne X, Leutwyler D, Osterried K, Panosetti D, Rüdissühli S, Schlemmer L, Schulthess T, Sprenger M, Ubbiali S, Wernli H (2020) Kilometer-scale climate models:

- prospects and challenges. *B Am Meteorol Soc* 101:E567–E587. <https://doi.org/10.1175/BAMS-D-18-0167.1>
- Skamarock WC, Klemp JB, Dudhia J, Gill DO, Liu Z, Berner J, Wang W, Powers JG, Duda MG, Barker DM, Huang XY (2019) A description of the advanced research WRF version 4. NCAR Tech. Note NCAR/TN-556+STR, p 145
- Smith A, Lott N, Vose R (2011) The integrated surface database: recent developments and partnerships. *B Am Meteorol Soc* 92:704–708. <https://doi.org/10.1175/2011BAMS3015.1>
- Somot S, Ruti PM, The MedCORDEX Team (2011) The Med-CORDEX initiative: towards fully coupled Regional Climate System Models to study the Mediterranean climate variability, change and impact. https://www.medcordex.eu/somot_MedCORDEX_WCRP2011_Denver_oct2011.pdf. Accessed 10 Jan 2022
- Stiperski I, Ivančan-Picek B, Grubišić V, Bajić A (2012) Complex Bora flow in the lee of Southern Velebit. *Q J R Meteorol Soc* 138:1490–1506. <https://doi.org/10.1002/qj.1901>
- Torma C, Giorgi F, Coppola E (2015) Added value of regional climate modeling over areas characterized by complex terrain precipitation over the Alps. *J Geophys Res Atmos* 120:3957–3972. <https://doi.org/10.1002/2014JD022781>
- Tyrlis E, Lelieveld J (2013) Climatology and Dynamics of the Summer Etesian Winds over the Eastern Mediterranean. *JAS* 70:3374–3396. <https://doi.org/10.1175/JAS-D-13-035.1>
- Ulbrich U, Lionello P, Belušić D et al (2012) Climate of the Mediterranean: synoptic patterns, temperature, precipitation, winds, and their extremes. In: Lionello P (ed) *The Climate of the Mediterranean Region - From the Past to the Future*. Elsevier, Amsterdam, pp 301–346
- Van Meijgaard E, Van Ulft LH, Van De Berg WJ, Bosveld FC, Van Den Hurk BJM, Lenderink G, Siebesma AP (2008) The KNMI regional atmospheric model RACMO version 2.1, technical report 302. Technical report, De Bilt KNMI, The Netherlands. <http://bibliotheek.knmi.nl/knmipubTR/TR302.pdf>. Accessed 22 Feb 2022
- Večenaj Ž, Belušić D, Grubišić V et al (2012) Along-Coast features of bora-related turbulence. *Boundary-Layer Meteorol* 143:527–545. <https://doi.org/10.1007/s10546-012-9697-6>
- Zecchetto S, Cappa C (2001) The spatial structure of the Mediterranean Sea winds revealed by ERS-1 scatterometer. *Int J Remote Sens* 22:45–70. <https://doi.org/10.1080/014311601750038848>

Publisher's Note Springer Nature remains neutral with regard to jurisdictional claims in published maps and institutional affiliations.

Springer Nature or its licensor (e.g. a society or other partner) holds exclusive rights to this article under a publishing agreement with the author(s) or other rightsholder(s); author self-archiving of the accepted manuscript version of this article is solely governed by the terms of such publishing agreement and applicable law.

Authors and Affiliations

Andreina Belušić Vozila¹  · Danijel Belušić^{2,3} · Maja Telišman Prtenjak² · Ivan Güttler⁴ · Sophie Bastin⁵ · Erwan Brisson⁶ · Marie-Estelle Demory⁷ · Andreas Dobler⁸ · Hendrik Feldmann⁹ · Øivind Hodnebrog¹⁰ · Stergios Kartsios¹¹ · Klaus Keuler¹² · Torge Lorenz¹³ · Josipa Milovac¹⁴ · Emanuela Pichelli¹⁵ · Mario Raffa¹⁶ · Pedro M. M. Soares¹⁷ · Merja H. Tölle¹⁸ · Heimo Truhetz¹⁹ · Hylke de Vries²⁰ · Kirsten Warrach-Sagi²¹

¹ Institute of Agriculture and Tourism, Karla Huguesa 8, 52440 Poreč, Croatia

² Department of Geophysics, Faculty of Science, University of Zagreb, Zagreb, Croatia

³ Swedish Meteorological and Hydrological Institute (SMHI), Norrköping, Sweden

⁴ Croatian Meteorological and Hydrological Service (DHMZ), Zagreb, Croatia

⁵ LATMOS/IPSL, UVSQ Université Paris-Saclay, CNRS, Sorbonne Université, Guyancourt, France

⁶ Groupe de Météorologie de Grande Échelle et Climat (GMGEC), Centre National de Recherches Météorologiques (CNRM), Université de Toulouse, Météo-France, Centre National de la Recherche Scientifique (CNRS), Toulouse, France

⁷ Institute for Atmospheric and Climate Science, ETH Zürich, Zurich, Switzerland

⁸ Norwegian Meteorological Institute, Oslo, Norway

⁹ Institute of Meteorology and Climate Research, Karlsruhe Institute of Technology (KIT), Karlsruhe, Germany

¹⁰ CICERO Center for International Climate Research, Oslo, Norway

¹¹ Department of Meteorology and Climatology, School of Geology, Aristotle University of Thessaloniki, Thessaloniki, Greece

¹² Brandenburg University of Technology Cottbus–Senftenberg, Cottbus, Germany

¹³ NORCE Norwegian Research Centre, Bjerknes Centre for Climate Research, Bergen, Norway

¹⁴ Instituto de Física de Cantabria, Universidad de Cantabria-CSIC, Santander, Spain

¹⁵ Earth System Physics (ESP), The Abdus Salam International Centre for Theoretical Physics (ICTP), Trieste, Italy

¹⁶ Regional Models and Geo-Hydrological Impacts (REMHI) Division, Fondazione Centro Euro-Mediterraneo Sui Cambiamenti Climatici, Caserta, Italy

¹⁷ Instituto Dom Luiz - University of Lisbon, Lisbon, Portugal

¹⁸ University of Kassel, Kassel Institute for Sustainability (KIS), Kassel, Germany

¹⁹ Wegener Center for Climate and Global Change (WEGC), University of Graz, Graz, Austria

²⁰ Royal Netherlands Meteorological Institute (KNMI), De Bilt, The Netherlands

²¹ Institute of Physics and Meteorology, University of Hohenheim, Stuttgart, Germany